The *Tight Skin* Mouse: Demonstration of Mutant Fibrillin-1 Production and Assembly into Abnormal Microfibrils

Cay M. Kielty,* Michael Raghunath,‡ Linda D. Siracusa,§ Michael J. Sherratt,* Reiner Peters,‖ C. Adrian Shuttleworth,* and Sergio A. Jimenez§

*School of Biological Sciences, University of Manchester, Manchester, M13 9PT, United Kingdom; ‡Department of Dermatology, ‖Department of Medical Physics and Biophysics, University of Muenster, D-48149, Germany; and Department of Microbiology and Immunology, §Department of Medicine, Jefferson Medical College, Thomas Jefferson University, Philadelphia, Pennsylvania 19107-5541

Abstract. Mice carrying the *Tight skin* (*Tsk*) mutation harbor a genomic duplication within the fibrillin-1 (*Fbn 1*) gene that results in a larger than normal in-frame *Fbn 1* transcript. In this study, the consequences of the *Tsk* mutation for fibrillin-containing microfibrils have been examined. Dermal fibroblasts from *Tsk*/+ mice synthesized and secreted both normal fibrillin ($\sim$330 kD) and the mutant oversized *Tsk* fibrillin-1 ($\sim$450 kD) in comparable amounts, and *Tsk* fibrillin-1 was stably incorporated into cell layers. Immunohistochemical and ultrastructural analyses of normal and *Tsk*/+ mouse skin highlighted differences in the gross organization and distribution of microfibrillar arrays. Rotary shadowing of high M_r preparations from *Tsk*/+ skin demonstrated the presence of abundant beaded microfibrils. Some of these had normal morphology and periodicity, but others were distinguished by diffuse interbeads, longer periodicity, and tendency to aggregate. The presence of a structurally abnormal population of microfibrils in *Tsk*/+ skin was unequivocally demonstrated after calcium chelation and in denaturing conditions. Scanning transmission electron microscopy highlighted the presence of more mass in *Tsk*/+ skin microfibrils than in normal mice skin microfibrils. These data indicate that *Tsk* fibrillin-1 polymerizes and becomes incorporated into a discrete population of beaded microfibrils with altered molecular organization.

T HE glycoprotein fibrillin-1 is the major structural protein of a widely distributed class of connective tissue microfibrils that are key components of elastic fibers (3, 23, 33, 34). The primary structure of fibrillin-1 predicts a M_r of 312,000 and a complex multidomain organization (4, 26). It contains 47 epidermal growth factor–like domains, 43 of which have calcium-binding consensus sequences (cbEGF[1]-like domains), 9 8-cysteine repeats, a proline-rich region that may act as a hinge, and unique amino- and carboxy-terminal sequences. Recently, a genomic duplication of 30–40 kb within the mouse *fibrillin 1* (*Fbn 1*) gene was described in association with the mouse *Tight skin* (*Tsk*) phenotype (37). This mutation results in a

mutant transcript that is 3 kb larger than the wild-type transcript, contains an in-frame duplication of exons 17–40, and is predicted to encode a mutant fibrillin-1 polypeptide of M_r 418,000. The mutant molecule would have an additional Arg-Gly-Asp (RGD) cell recognition sequence, two and one-third additional 8-cysteine repeats, 18 additional cbEGF-like domains, and one extra hybrid 8-cysteine motif, in comparison to the wild-type fibrillin-1 protein.

The phenotype of heterozygous *Tsk*/+ mice includes thickened skin and visceral fibrosis resulting from accumulation of extracellular matrix (10). The skin adheres firmly to the hyperplastic subcutaneous tissues, lacks the pliability and elasticity of normal skin, and exhibits altered wound healing properties. Other features include increased bone and cartilage growth, lung emphysema, myocardial hypertrophy, and the presence of small tendons with tendon sheath hyperplasia (7, 21, 31). Large accumulations of microfibrils, several collagens, and glycosaminoglycans have been identified in various *Tsk*/+ organs including skin, heart, and lungs (10, 13, 14). Homozygous *Tsk* embryos degenerate at 7 or 8 d of development, whereas heterozygous mice have a normal life span. The *Tsk* mouse

Address all correspondence to Cay M. Kielty, School of Biological Sciences, 2.205 Stopford Bldg., University of Manchester, Manchester M13 9PT, UK. Tel.: (44) 161-275-5739. Fax: (44) 161-275-5082. E-mail: cay. kielty@man.ac.uk

1. *Abbreviations used in this paper*: cbEGF, calcium-binding EGF; cys, cysteine; GuHCL, guanidinium chloride; *Fbn 1*, fibrillin 1 gene; met, methionine; MFS, Marfan syndrome; STEM, scanning transmission electron microscopy; *Tsk*, Tight skin mutation.

This document was created with FrameMaker 4.0.4

has been used as a model for several human diseases, including cardiac hypertrophy (15, 25), hereditary emphysema (7, 22, 32) and systemic sclerosis or scleroderma (15). The *Tsk* phenotype may arise as a direct consequence of microfibril structural defects resulting from the mutation in *Fbn 1* and/or by alterations in cellular activity induced by the mutation. Comparable steady-state levels of normal and mutant *Fbn 1* transcripts in *Tsk*/+ tissues (37) and abundant amounts of tissue microfibrils (10) suggest that mutant *Tsk* fibrillin-1 is synthesized and assembled. The disorganization and fragmentation of *Tsk*/+ elastic fibers (7) may reflect structurally abnormal microfibrils.

Rotary shadowing analyses of fibrillin-containing microfibrils have demonstrated pronounced beaded domains connected by filamentous interbead regions, a regular diameter of 10–12 nm, and an average axial periodicity, in relaxed isolated state of 50–56 nm (17, 18, 36). Polymerized fibrillin forms the structural framework of microfibrils, but key details that remain outstanding are the arrangement of fibrillin monomers within microfibrils and the molecular basis of microfibril diameter, periodicity, and extensibility. The purpose of this study was to demonstrate the synthesis of abnormal mutated fibrillin-1 molecules in *Tsk*/+ mice and to examine their incorporation into skin microfibrils to generate new insights into microfibril assembly and organization.

Materials and Methods

Materials

Bacterial collagenase (type 1A), PMSF, *N*-ethylmaleimide (NEM), benzamidine, guanidinium chloride (GuHCl), protein A–Sepharose colloidal gold conjugate, protein A–Sepharose, and Triton X-100 were obtained from Sigma Chemical Co. (Poole, Dorset, UK). Sepharose CL-2B was supplied by Pharmacia-LKB (Milton Keynes, Bucks, UK). MultiMark™ SDS-PAGE molecular weight markers were supplied by Novex (San Diego, CA). Normal donkey serum and Texas red were purchased from Jackson ImmunoResearch (West Grove, PA), and Mowiol was purchased from Hoechst, (Frankfurt-Hoechst, Germany). ^{35}[S]cys/met Translabel and ^{45}CaCl$_2$ was obtained from ICN Biomedicals, Inc., (Meckenheim, Germany). Chelex 100 was obtained from (Bio-Rad Laboratories, Hercules, CA). The antifibrillin antisera used were a polyclonal antibody (9022) raised to fibrillin-1 PF2 fragment (20) that was kindly provided by R. Glanville (Shriner's Hospital, Portland, OR) and a polyclonal antibody (5077) raised to intact microfibrils (17, 20, 27).

Mice

Mice of the C57BL/6-*pa* +/+*Tsk* genotype were originally purchased from Jackson Laboratory (Bar Harbor, ME). The *Tsk* mutation was transferred onto the C57BL/6J (B6) background by sequential backcrossing at the Jefferson Medical College (Philadelphia, PA). The B6-*Tsk*/+ and B6-+/+ mice used for these studies were at the N6 generation. The mutant *Tsk* phenotype was determined by manual assessment of the thickness and tightness of the skin in the intercapsular region as well as by Southern blot analyses to distinguish the presence or absence of the duplicated region of the *Fbn 1* gene (37).

Biosynthesis and Radioimmunoprecipitation of Fibrillin

Dermal fibroblasts were established from normal and *Tsk*/+ mice and were seeded at a density of 5×10^5 per 35-mm dish after passage. When confluent, the cultures were either labeled continuously in the presence of 100 μCi of ^{35}[S]cys/met per 0.5ml cys- and met-free minimal essential medium per well for 17 h, or pulse labeled with 100 μCi ^{35}[S]cys/met for 60 min, and then chased for 24 h. Fibrillin was radioimmunoprecipitated from the continuously labeled culture medium, which was preabsorbed with normal rabbit serum and protein A–Sepharose overnight at 4°C. Af-

ter removal of Sepharose beads, the media were incubated with the PF2 antibody or normal rabbit serum (25 μl per 0.5-ml aliquot) for 19 h at 4°C. Immune complexes were adsorbed to a suspension of 50 μl of protein A–Sepharose for 2 h at room temperature and then washed three times in radioimmunoprecipitation assay buffer. The bound proteins were released by boiling in 75 μl of double-strength sample buffer containing 10% β-mercaptoethanol. Proteins were separated on 4% SDS-PAGE gels. Aliquots of crude medium were added to equal volumes of double-strength sample buffer and then analyzed on the same gel (27).

Confocal Laser Scanning Immunolabeling Analysis

Cryostat sections (7 μm) of normal and *Tsk*/+ mice skin were fixed in acetone for 10 min. Nonspecific binding sites were blocked by incubation with 10% normal donkey serum/1% BSA in PBS for 30 min at room temperature. This step was followed by incubation in primary antibody (PF2 antibody or 5507; 1:100 in PBS) overnight at room temperature. Bound antibody was visualized using a 1:100 dilution of donkey Fab2 against rabbit IgG coupled to Texas red for 30 min at room temperature. Preparations were mounted in Mowiol in 0.01 M Tris-HCl, pH 8.6. Preparations were examined using an invert device (model LSM 410; Carl Zeiss, Inc., Oberkochen, Germany). A 40-fold oil immersion objective (numerical aperture 1.3) was used. Single optical sections (0.6–0.7 μm) were obtained with identical scanning settings and excitation conditions to distinguish differences in fluorescence intensities between *Tsk*/+ and normal mouse skin.

Transmission Electron Microscopy

Skin biopsies were minced, fixed in 2.5% glutaraldehyde in 100 mM cacodylate, pH 7.2, for 48 h, osmicated en bloc, and then embedded in Epon 812 (Polysciences Inc., Warington, PA). Ultrathin sections were counterstained with uranyl acetate and lead citrate and then viewed with an electron microscope (model EM 401; Philips Electron Optics, Eindhoven, The Netherlands) at an accelerating voltage of 60 kV.

Isolation of Intact Fibrillin-containing Microfibrils

Triplicate preparations of intact native microfibrils were isolated from normal and *Tsk*/+ mouse skin using a well-defined methodology (17, 19, 36). Briefly, tissues were disrupted by bacterial collagenase digestion in 0.05 M Tris-HCl, pH 7.4, containing 0.4 M NaCl and 0.01 M CaCl$_2$ in the presence of proteinase inhibitors (5 mM PMSF, 2 mM NEM, 5 mM benzamidine). Microfibrils were isolated as high M_r assemblies in the void volume of a Sepharose CL-2B gel filtration chromatography column (15 × 1 cm; Pharmacia Biotech Ltd., Herts, UK). All microfibril preparations were examined directly by rotary shadowing–electron microscopy and scanning transmission electron microscopy (STEM). Microfibrils were incubated for various lengths of time at 20°C in 5 mM EDTA or 5 mM CaCl$_2$, or at 37°C in 4 M GuHCl.

Enzymatic Digestion of Microfibrils

A suspension of intact microfibrils was equilibrated in 0.025 M Tris-HCl, pH 7.4, containing 0.2 M NaCl with or without 5 mM EDTA and then incubated for 2 or 18 h at 37°C in the presence of trypsin (Sigma Chemical Co.) (1 μg:100 μl) or neutrophil elastase (gift from D. Woolley, University of Manchester, Manchester, UK) (100 ng:100 μl). Consequences for microfibril integrity were monitored by rotary shadowing.

Rotary Shadowing–Electron Microscopy

Preparations of intact microfibrils were adsorbed directly onto carbon-coated grids (2–3-nm film thickness) and metal shadowed with a tungsten/platinum filament at an angle of 4° (17, 36). Grids were visualized using an electron microscope (model 1200EX; JEOL USA, Inc., Peabody, MA) at an accelerating voltage of 100 kV.

STEM

STEM mass analysis is a well-established technique that has provided quantitative data on mass per unit length and axial mass distribution on unstained and unshadowed fibrillin-containing microfibrils and other macromolecules (11, 12, 24, 35, 36). Preparations of intact native microfibrils were analyzed by STEM in a JEOL 1200EX transmission electron microscope as previously described (36). Mean axial repeat measurements for each microfibril preparation were calculated from 40–50 axial

repeat measurements across 10–30 periods per microfibril, with an error of ±0.34%. Five measurements of mass per unit length were taken per microfibril, with 40–50 microfibrils per grid examined. Axial mass distributions were averages involving 10 measurements per microfibril. In all cases, these STEM measurements were repeated on triplicate preparations. The axial repeat was the distance from the beginning of one bead to the beginning of the next (effectively one bead plus one interbead domain). Analysis of variance analysis of axial repeat, mass per unit length, and total mass per axial repeat data was performed.

Results

Synthesis and Secretion of Fibrillin-1 by Tsk/+ Dermal Fibroblasts

Metabolic labeling of normal mouse dermal fibroblasts and subsequent SDS-PAGE under reducing conditions revealed a single protein band of ~330 kD that comigrated with fibrillin from normal human fibroblasts (data not shown) and was identified by the PF2 antibody (Fig. 1 A). In contrast, the Tsk/+ dermal fibroblast culture medium contained an additional protein of ~450 kD that was also recognized by these antibodies and was therefore identified as the gene product of the larger mutant Tsk Fbn 1 gene. Bands corresponding to normal and Tsk fibrillin-1 in the Tsk/+ fibroblast radioimmunoprecipitates were of comparable intensity. No specific protein bands were immunoprecipitated with normal rabbit serum. Pulse-chase analysis revealed that Tsk fibrillin-1 could be recovered from the extracellular matrix of the fibroblast cultures (Fig. 1 B).

Confocal Laser and Transmission Electron Microscopy Analysis of Fibrillin-1 in Tsk/+ Mice Skin

A confocal laser scanning analysis of immunostaining of the cutaneous microfibrillar network appeared substantially more intense in the Tsk/+ skin than in the normal mouse with the PF2 antibody, and far more details of this structure were discernible (Fig. 2 A). In contrast, the antibody 5507 immunostained microfibrils in both normal and mutant mice, but the immunostaining intensity was lower in the Tsk/+ mouse under identical scanning conditions (Fig. 2 B). This difference was most pronounced with the microfibrils around hair follicles.

A transmission electron microscopy study revealed that, in comparison with normal mice, Tsk/+ mice skin had more prominent microfibrillar "clusters" in the upper dermis, although there was a noticable absence of well-packed elastic fibrils with very electron-dense cores (Fig. 3). Tsk/+ mouse microfibrils, with or without associated elastin, frequently appeared blurred without a discernible striated pattern. The elastin appeared less electron dense and less compact than those in samples from normal animals.

Examination of Microfibrils Isolated from Tsk/+ Mice Skin

Ultrastructure. Abundant beaded microfibrils were isolated from littermate pairs of normal and Tsk/+ mice skin (Fig. 4, A and B). Microfibrils from normal mouse skin were well-organized linear arrays (Fig. 4 A). Some microfibrils isolated from Tsk/+ skin were morphologically similar to those of the normal animals, but many other Tsk/+ skin microfibrils were abnormal periodic arrays of beads with indistinct filamentous interbeads and extended
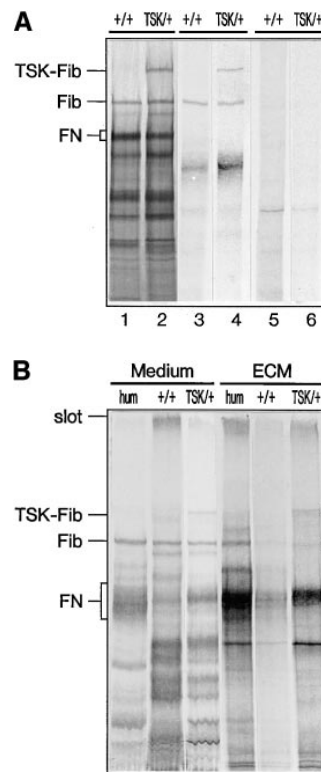

Figure 1. (A) SDS-PAGE analysis of newly synthesized fibrillin-1 radioimmunoprecipitated from normal and Tsk/+ dermal fibroblast cultures. Newly synthesized, labeled fibrillin-1 was radioimmunoprecipitated from the medium of dermal fibroblasts that had been labeled with ^{35}[S]cys/met for 17 h. Tsk/+ cells synthesized and then secreted both normal (~330 kD) and Tsk fibrillin-1 (~450 kD) in comparable amounts. Lanes 1, 3 and 5, medium from normal mice cells; lanes 2, 4, and 6, medium from Tsk/+ mice cells. Lanes 1 and 2, crude medium; lanes 3 and 4, fibrillin-1 immunoprecipitated with PF2 antiserum; lanes 5 and 6, immunoprecipitation controls using normal rabbit serum. (B) Incorporation of the oversized Tsk monomer into extracellular matrix. Normal and Tsk fibroblast cultures were pulsed for 1 h with ^{35}[S]met/cys and chased in culture medium containing 2% fetal calf serum for 24 h. Medium and extracellular matrix extracts were harvested after this period of time. The medium and extracellular matrix of both cell cultures contains the normal fibrillin (~330 kD). (small arrow). In addition, medium and extracellular matrix of the Tsk cell strain contain the oversized fibrillin-1 monomer (~450 kD; large arrow).

periodicity (Fig. 4 B). The axial periodicity of control mice microfibrils and the apparently normal population of microfibrils in Tsk/+ preparations was 55 ± 4 nm, which is comparable to previously published dimensions of microfibrils from other sources (18, 36). However, the abnormal Tsk/+ skin microfibrils had a more extended bead-to-bead distance of 112 ± 11 nm. The number of normal and abnormal microfibrils in triplicate Tsk/+ skin preparations was counted in 200 low-magnification (5,000×) fields; this analysis indicated that the abnormal microfibrils represented 45 ± 10% of the total microfibril population.

Aggregates. Extensive microfibril clusters were also present in the Tsk/+ skin preparations, but not in those from normal skin (Fig. 5, A and B). In these aggregates, intermicrofibril filaments were apparent.

STEM Mass Analysis. STEM mass analysis in dark field of normal and Tsk/+ skin microfibrils detected a significant mass increase in the Tsk/+ skin microfibril population. Total mass per axial repeat for the normal skin microfibrils was 2,547 kD, whereas that for the abnormal Tsk/+ skin microfibrils was 3,074 kD, an average increase of 527 kD per axial repeat.

Stability of Tsk/+ Skin Microfibrils

Structural Response to Calcium Chelation. Rotary shadowing examination of normal mouse skin microfibrils incu-
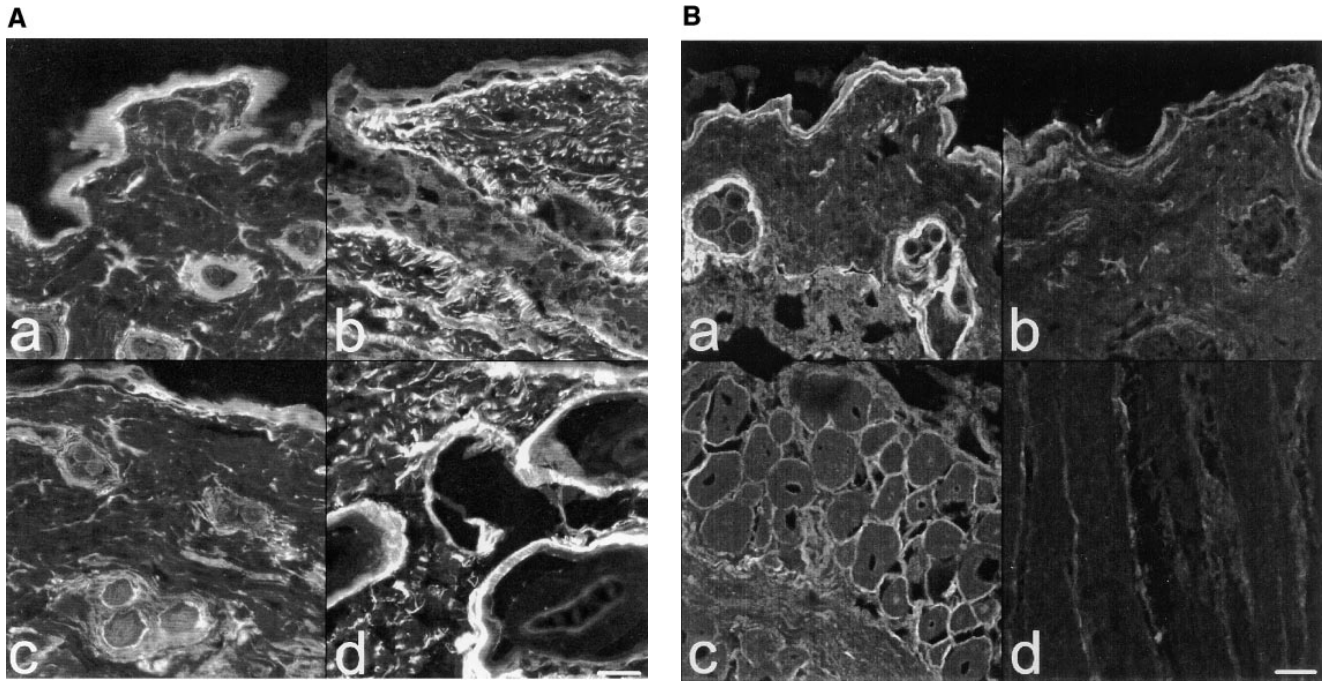
A

B

Figure 2. Confocal laser scanning analysis of normal and *Tsk*/+ mice skin. (*A*) *a* and *c*, normal mouse skin; *b* and *d*, *Tsk*/+ mouse skin. In the normal mouse, PF2 antibody stains the papillary microfibrillar apparatus beneath and along the basement membrane region, perivascular microfibrils, and the surrounding microfibrillar matrix around hair follicles. The identical regions in the *Tsk*/+ mouse are labeled, but in comparison with normal mouse skin, the intensity of the immune signal is substantially increased. Bar, 20 μm. (*B*) *a* and *c*, normal mouse; *b* and *d*, *Tsk*/+ mouse. In the normal mouse, 5507 antibody strongly stains the papillary microfibrillar apparatus beneath the dermal–epidermal junction and the matrix surrounding the hair follicles. The same structures are immunolabeled in *Tsk*/+ skin, but the intensity is reduced. Bar, 20 μm.

bated in the presence of 5 mM EDTA for 10 min demonstrated they had reduced periodicity (38 ± 2 nm), prominent beads, and a diffuse interbead appearance as previously described (35) (Fig. 4 *C*). The morphologically normal microfibrils from *Tsk*/+ skin exhibited the same response as the normal mouse skin microfibrils to calcium chelation (Fig. 4 *D*). However, EDTA-induced changes in the abnormal *Tsk*/+ skin microfibril population were unequivocally different from those of the apparently normal microfibrils (Fig. 4 *D*). Axial repeat distances in the abnormal microfibrils were reduced to 61 ± 3 nm, and beads did not appear prominent, although interbeads became more indistinct. EDTA failed to disrupt the large *Tsk*/+ microfibril aggregates that remained tightly associated but with less well-defined intermicrofibril filaments (Fig. 5, *C* and *D*).

Effects of Chaotropic Agents. To study whether *Tsk*/+ mice skin microfibrils had altered stability, the effects of chaotropic agents were assessed. 4 M GuHCl-treated normal mice skin microfibrils and the apparently normal *Tsk*/+ skin microfibrils underwent a conformational change similar to that observed for EDTA, with periodicities reduced to 43.9 ± 9.2 nm, although they remained beaded polymers as previously reported for bovine microfibrils (36). In contrast, the abnormal *Tsk*/+ microfibrils became disordered networks with loss of overt periodicity (data not shown).

Susceptibility to Enzymatic Digestion. In the presence of calcium, microfibrils isolated from normal and *Tsk*/+ mice were degraded to short, beaded arrays by trypsin or neu-

trophil elastase by 18 h. There were no obvious differences in the susceptibility of the control mice microfibrils and the morphologically normal *Tsk*/+ skin microfibrils to degradation by either enzyme. Short arrays of normal and abnormal *Tsk*/+ skin microfibrils were detected after digestion, as judged by morphology (data not shown). When EDTA-treated microfibrils were incubated with enzymes, all microfibrils were rapidly degraded within 2 h, with only beaded domains apparent.

Discussion

A previous study of *Tsk* mice demonstrated that a tandem duplication within the *Fbn 1* is associated with the mouse *Tsk* mutation and established that the mutant allele is transcribed in *Tsk* tissues (37). This investigation was undertaken to study whether *Tsk* fibrillin-1 protein is produced and assembled, and if so, to examine the consequences for microfibril organization.

The *Tsk* mutation is predicted to give rise to an oversized fibrillin-1 molecule with a calculated molecular mass of 418 kD (37) and an expected presence of seven potential additional *N*-glycosylation sites. We demonstrate now that cultured dermal fibroblasts of *Tsk*/+ mice synthesize and secrete normal fibrillin-1 with an apparent molecular mass of 330 kD and a fibrillin-1 molecule with an apparent molecular mass of 450 kD in comparable amounts. The electrophoretic behavior of *Tsk* fibrillin-1 was in accordance with the predictions and confirmed full expression
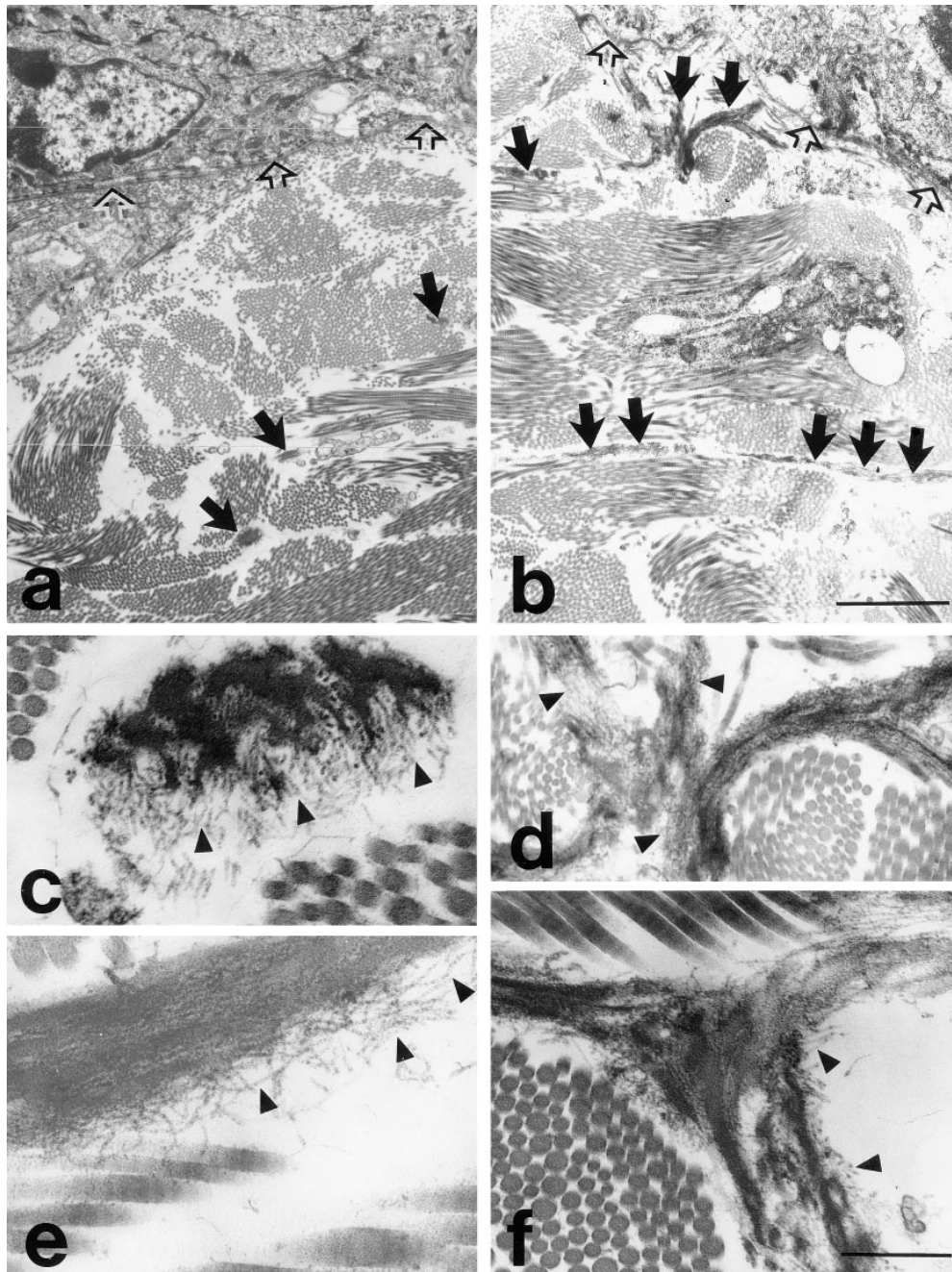
Figure 3. Ultrastructural study of normal and *Tsk/+* mice skin. *a*, *c*, and *e*, normal mouse; *b*, *d*, and *f*, *Tsk/+* mouse. *a* and *b* are low-power views (5,000×) showing basal keratinocytes, the dermo–epidermal junction as represented by the lamina densa (*open arrows*), and the upper dermis. In both mice, the dermis is dominated by collagen bundles. Microfibrillar bundles and elastic fibers are indicated by closed arrows. *b* reveals the presence of larger microfibrillar bundles with abundant microfibrils but little elastin. *c–f* are high magnification views of elastic fibers and microfibrillar bundles. These appear less well defined in *Tsk/+* skin (*d* and *f*) than in normal skin (*c* and *e*). In particular, the striation pattern of microfibrils (*arrowheads*) seen with the normal animals (*c* and *e*) was less apparent in the *Tsk/+* mice skin. Bars: (*a* and *b*) 3,000 nm; (*c–f*) 250 nm.

of the mutant protein. We have several lines of evidence that this oversized molecule aggregates and is incorporated into microfibrils.

Pulse-chase experiments confirmed the incorporation of comparable levels of newly synthesized normal and oversized fibrillin-1 monomers into the extracellular matrix of *Tsk* dermal fibroblast cultures. Confocal laser scanning microscopy confirmed the presence of a cutaneous microfibrillar network in *Tsk* mice. Immunoreactivity differences to normal mice using antibodies raised to fibrillin-1 and to intact microfibrils could reflect altered microfibril abundance, changed accessibility of fibrillin-1 epitopes, and/or secondary extracellular matrix changes in affected mice. The transmission electron microscopy study demonstrated that *Tsk/+* skin microfibrils were blurred in ap-

pearance with no obvious periodicity and limited elastin deposition, indicating structural microfibrillar changes.

Ultrastructural examination of beaded microfibrils isolated from *Tsk/+* skin revealed clear evidence for two distinct microfibril populations, one composed of morphologically normal microfibrils, whereas the other population of microfibrils was abnormal with diffuse interbeads and longer than normal periodicity. No other microfibrils with such structural characteristics have previously been demonstrated from any tissue or cellular source. These observations indicate that the abnormal microfibrils compose *Tsk* fibrillin-1 and have consequently altered molecular organization. The dark-field STEM data demonstrating increased mass of *Tsk/+* skin microfibrils support this conclusion. The extra mass presumably reflects incorporation
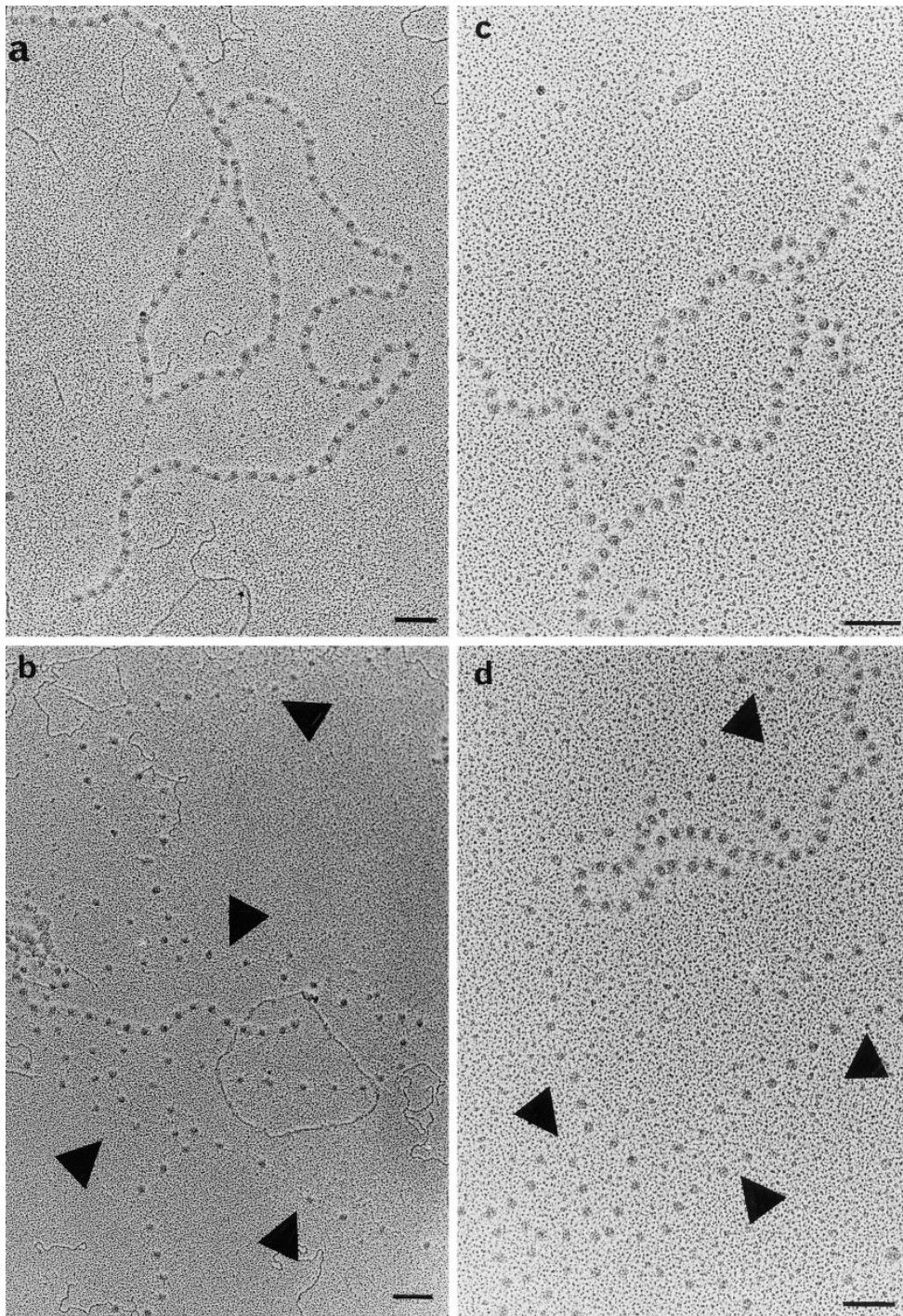
Figure 4. Rotary shadowing analysis of normal and *Tsk/+* skin microfibrils. *a* and *c*, normal skin microfibrils; *b* and *d*, *Tsk/+* skin microfibrils. (*a*) Normal mice skin microfibrils exhibited well-organized packing and regular diameter. (*b*) *Tsk/+* mice skin microfibrils. Some appeared normal in morphology and periodicity, whereas others appeared as periodic rows of beads with indistinct interbeads and repeat distances longer than normal (*arrowheads*). (*c*) Normal mice skin microfibrils after incubation for 10 min in 5 mM EDTA. (*d*) *Tsk/+* mice skin microfibrils after incubation for 10 min in 5 mM EDTA. The apparently normal microfibrils responded to EDTA as control mice microfibrils, but the abnormal microfibrils remained morphologically distinct (*arrowheads*). Grids were examined using a JEOL 1200EX electron microscope at an accelerating voltage of 100 kV. Bars, 100 nm.

of the larger than normal *Tsk* fibrillin-1 molecules in the abnormal microfibril pool, although the involvement of other microfibril-associated molecules cannot be excluded (1, 8, 9, 18, 19, 36, 39). The large microfibrillar clusters that further distinguished the *Tsk/+* skin microfibril preparations appeared to contain the abnormal microfibrils that presumably have altered surface interactive properties. Structural differences between morphologically normal and abnormal *Tsk/+* mice skin microfibrils were confirmed in calcium chelation experiments in which the appearance and periodicity of abnormal *Tsk/+* skin microfibrils was fundamentally different from those of the morphologically normal microfibrils in these preparations. Removal of calcium from normal microfibrils and fibrillin-1 molecules causes molecular shortening, increased mass per unit length, and conformational changes (16, 30, 35). Periodicity of abnormal *Tsk/+* microfibrils is reduced, although the beads do not appear prominent like those of EDTA-treated control microfibrils; this distinct response is probably due to misalignment, misfolding, or aberrant cross-linking.

The data obtained with *Tsk/+* skin microfibrils show that *Tsk* fibrillin-1 is produced, assembled, and deposited
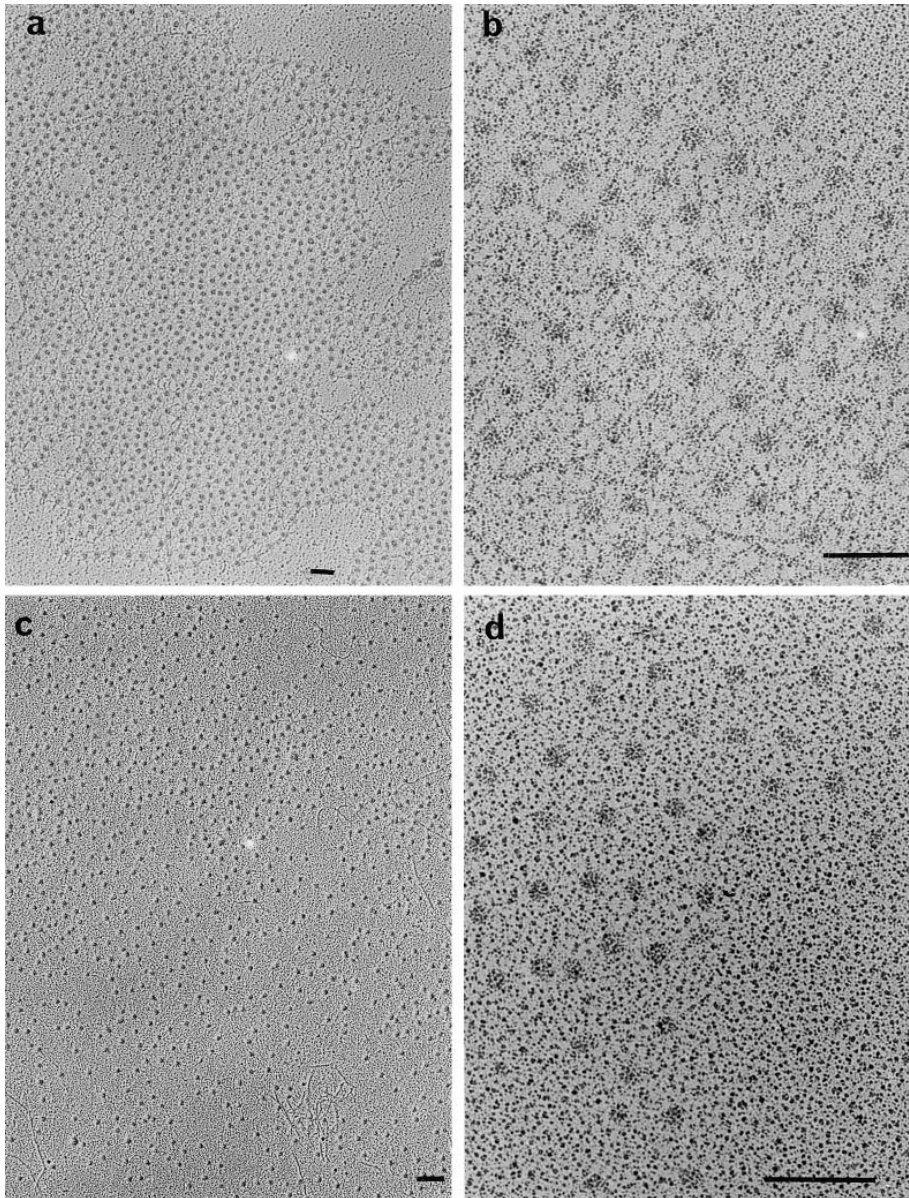
Figure 5. Rotary shadowing analysis of microfibrillar aggregates isolated from *Tsk/+* skin. Numerous extensive microfibril clusters were present in the *Tsk/+* skin preparations. (*a* and *b*) Microfibril clusters after isolation in native, calcium-containing state. (*c* and *d*) Microfibril clusters after 10-min incubation in 5 mM EDTA. Grids were examined using a JEOL 1200EX electron microscope at an accelerating voltage of 100 kV. Bars, 100 nm.

in the extracellular matrix, and that abnormal beaded *Tsk* fibrillin-1 microfibrils with longer than normal periodicity and altered morphology and organization are present in *Tsk/+* skin. The experiments indicate the occurrence of mutually exclusive normal and mutant fibrillin-1 homopolymeric beaded microfibrils and highlight that microfibril periodicity directly reflects monomer length. The data demonstrate a requirement for fibrillin molecules of similar length for copolymerization into microfibrils. The extended internal sequence of *Tsk* fibrillin-1 does not preclude homopolymer assembly, and primary nucleation roles for the unchanged amino- and carboxy-terminal sequences in assembly are indicated. Molecular selection based on length suggests that lateral alignment of fibrillin molecules is a crucial assembly step and may precede or facilitate linear polymerization. Current models of fibrillin alignment, based on measured molecular dimensions and antibody epitope mapping (29), or extrapolation of molecular length based on cbEGF-like domain dimensions (6), suggest a parallel alignment of fibrillin monomers, although whether the monomers are unstaggered is not resolved. The extended periodicity that results from polymerization of *Tsk* fibrillin-1 molecules supports an unstaggered arrangement.

Abnormal *Tsk* fibrillin-1 microfibrils and aggregated clusters presumably contribute to the *Tsk* phenotype. Mutations of the human counterpart to the *Fbn 1* gene, the FBN 1 locus on chromosome 15q (28), lead to a distinct phenotype, the Marfan syndrome (MFS), an autosomal dominant disorder characterized by pleiotropic connective tissue defects and life-threatening vascular complications. The dominant-negative effects of MFS reflects reduced levels of competent microfibrils in MFS patient tissues and cell cultures (17, 28) and indicates that copolymerization of normal and mutant allele products is universally disruptive to microfibril structure and function. The *Tsk* fibrillin-1 mutation may not predispose to tissue and vascular alterations precisely because stable heteropolymers of both normal and *Tsk* fibrillin-1 cannot form, with the normal

fibrillin-1 microfibril population able to sustain normal vascular development and functional elastic fiber formation. Altered growth factor binding potential, either through duplicated fibrillin-1 8-cysteine motifs or altered microfibril association with latent transforming growth factor binding proteins (8, 38), may contribute to the characteristic up-regulation of extracellular matrix molecules in *Tsk* mice. It is interesting to speculate that human disorders such as congenital facial dystrophy or restrictive dermopathy (5, 39), characterized by excess collagen deposition and "tight" skin, could have a similar aetiology to the *Tsk* phenotype.

References

1. Chan, F.L., and H.L. Choi. 1995. Proteoglycans assocated with the ciliary zonule of the rat eye: a histochemical and immunocytochemical study. *Histochem. Cell Biol.* 104:369–381.

2. Chapman, D., and M. Eghbali. 1990. Expression of fibrillar types I and III and basement membrane collagen type IV genes in myocardium of tight skin mouse. *Cardiovasc. Res.* 24:578–583.

3. Cleary, E.G., and M.A. Gibson. 1983. Elastin-associated microfibrils and microfibrillar proteins. *Int. Rev. Connect. Tiss. Res.* 10:97–209.

4. Corson G.M., S.C. Chalberg, H.C. Dietz, N.L. Charbonneau, and L.Y. Sakai. 1993. Fibrillin binds calcium and is coded by cDNAs that reveal a multidomain structure and alternatively spliced exons at the 5′ end. *Genomics.* 17:476–484.

5. Das-Kundu, S., H.H. Klunemann, D. Mieth, M. Spycher, T. Stallmach, and A. Schinzel. 1996. Case of the month: a newborn with tight skin and joint contractures. *Eur. J. Pediatr.* 155:987–989.

6. Downing, A.K., V. Knott, J.M. Werner, C.M. Cardy, I.D. Campbell, and P. Handford. 1996. Solution structure of a pair of Ca^{2+} binding epidermal growth factor-like domains: implications for the Marfan syndrome and other genetic disorders. *Cell.* 85:597–605.

7. Gardi, C., P.A. Martorana, M.M. de Santi, P. van Even, and G. Lungarella. 1989. A biochemical and morphological investigation of the early development of genetic emphysema in tight-skin mice. *Exp. Mol. Pathol.* 50:398–410.

8. Gibson, M.A., G. Hatzinikolas, E.C. Davis, E. Baker, G.R. Sutherland, and R.P. Mecham. 1995. Bovine latent transforming growth factor β 1-binding protein 2: molecular cloning, identification of tissue isoforms, and immunolocalisation to elastin-associated microfibrils. *Mol. Cell. Biol.* 15:6932–6942.

9. Gibson, M.A., G. Hatzinikolas, J.S. Kumaritilake, L.S. Sandberg, J.K. Nicholl, G.R. Sutherland, and E.G. Cleary. 1996. Further characterisation of proteins associated with elastic fiber microfibrils including the molecular cloning of MAGP-2 (MP25). *J. Biol. Chem.* 271:1096–1103.

10. Green, M.C., H.O. Sweet, and L.E. Bunker. 1975. Tight-skin, a new mutation of the mouse causing excessive growth of connective tissue and skeleton. *Am. J. Pathol.* 82:493–512.

11. Holmes, D.F., R.B. Watson, B. Steinmann, and K.E. Kadler. 1993. Ehlers-Danlos syndrome type VIIB. Morphology of type I collagen fibrils formed in vivo and in vitro is determined by the conformation of the retained N-propeptide. *J. Biol. Chem.* 268:15758–15765.

12. Holmes, D.F., A.P. Mould, and J.A. Chapman. 1991. Morphology of sheet-like assemblies of pN-collagen, pC-collagen and procollagen studied by scanning transmission electron microscopy mass measurements *J. Mol. Biol.* 220:111–123.

13. Jimenez, S.A., A. Millan, and R.I. Bashey. 1984. Scleroderma-like alterations in collagen metabolism occurring in the TSK (tight-skin) mouse. *Arthritis Rheum.* 27:180–185.

14. Jimenez, S.A., C. Williams, J. Myers, and R.I. Bashey. 1986. Increased collagen biosynthesis and increased expression of type I and III collagen genes in tight-skin (TSK) mouse fibroblasts. *J. Biol. Chem.* 261:657–662.

15. Jimenez, S.A., R.I. Bashey, C. Williams, and A. Millan. 1988. The tight-skin (TSK) mouse as an experimental model of scleroderma. *In* Handbook of Animal Models for the Rheumatic Diseases. Vol. 1. R. Greenwald, and H. Diamond, editors. CRC Press. Boca Raton, FL 169–193.

16. Kielty, C.M., and C.A. Shuttleworth. 1993. The role of calcium in the organisation of fibrillin microfibrils. *FEBS Lett.* 336:323–326.

17. Kielty, C.M., and C.A. Shuttleworth. 1994. Abnormal fibrillin assembly by dermal fibroblasts from two patients with Marfan syndrome. *J. Cell Biol.* 124:997–1004.

18. Kielty, C.M., and C.A. Shuttleworth. 1995. Fibrillin-containing microfibrils: structure and function in health and disease. *Int. J. Biochem. Cell Biol.* 27:747–760.

19. Kielty, C.M., S.P. Whittaker, and C.A. Shuttleworth. 1996. Fibrillin: evidence that chondroitin sulphate proteoglycans are components of microfibrils and associate with newly-synthesised monomers. *FEBS Lett.* 386:169–173.

20. Maddox, B.K., L.Y. Sakai, D.R. Keene, and R.W. Glanville. 1989. Connective tissue microfibrils. Isolation and characterisation of three large pepsin-resistant domains of fibrillin. *J. Biol. Chem.* 264:21381–21385.

21. Martorana, P.A., P. van Even, C. Gardi, and G. Lungarella. 1989. A 16-month study of the development of genetic emphysema in tight-skin mice. *Am. J. Respir. Dis.* 139:226–232.

22. Martorana, P.A., M. Wilkinson, P. van Even, and P. Lungarella. 1990. TSK mice with genetic emphysema. *Am. Rev. Respir. Dis.* 142:333–337.

23. Mecham, R.P., and J.E. Heusar. 1991. The elastic fiber. *In* Cell Biology of the Extracellular Matrix, 2nd Edition. E.D. Hay, editor. Plenum Press, New York. 79–109.

24. Muller, S.A., K.N. Goldie, R. Burki, R. Haring, and A. Engel. 1992. Factors influencing the precision of quantitative scanning transmission electron microscopy. *Ultramicroscopy.* 46:317–334.

25. Osborn, T.G., R.I. Bashey, T.L. Moore, and U.W. Fisher. 1987. Collagenous abnormalities in the heart of the tight-skin mouse. *J. Mol. Cell. Cardiol.* 19:581–587.

26. Pereira, L., M. D'Alessio, F. Ramirez, J.R. Lynch, B. Sykes, T. Pangilinan, and J. Bonadio. 1993. Genomic organisation of the sequence coding for the fibrillin gene product in Marfan syndrome. *Hum. Mol. Genet.* 2:961–968.

27. Raghunath, M., C.M. Kielty, and B. Steinmann. 1995. Truncated profibrillin of a Marfan patient is of apparent similar size as fibrillin: intracellular retention leads to over N-glycosylation. *J. Mol. Biol.* 248:901–909.

28. Ramirez, F. 1996. Fibrillin mutations in Marfan syndrome and related phenotypes. *Curr. Opin. Genet. Dev.* 6:309–315.

29. Reinhardt, D.P., D.R. Keene, G.M. Corson, E. Poschl, H.-P. Bachinger, J. E. Gambee, and L.Y. Sakai. 1996. Fibrillin-1: organisation in microfibrils and structural properties. *J. Mol. Biol.* 258:104–116.

30. Reinhardt, D.P., R.N. Ono, and L.Y. Sakai. 1997. Calcium stabilises fibrillin-1 against proteolytic degradation. *J. Biol. Chem.* 272:1231–1236.

31. Ross, S.C., T.G. Osborn, R.W. Dorner, and J. Zuckner. 1983. Glycosaminoglycan content in the skin of the tight-skin mouse. *Arthritis Rheum.* 27:180–185.

32. Rossi, G.A., G.W. Hunninghake, J.E. Gadek, S.V. Szapiel, O. Kawanami, and V.J. Ferrans. 1984. Hereditary emphysema in the tight-skin mouse. *Am. J. Respir. Dis.* 129:850–855.

33. Sakai, L.Y., D.R. Keene, and E. Engvall. 1986. Fibrillin, a new 350-kD glycoprotein, is a component of extracellular microfibrils. *J. Cell Biol.* 103:2499–2509.

34. Sakai, L.Y., D.R. Keene, R.W. Glanville, and H.-P. Bachinger. 1991. Purification and partial characterisation of fibrillin, a cysteine-rich structural component of connective tissue microfibrils. *J. Biol. Chem.* 266:14763–14770.

35. Sherratt, M.J., D.F. Holmes, C.A. Shuttleworth, and C.M. Kielty. 1996. Fibrillin-containing microfibrils: STEM analysis reveals calcium-dependent alterations in mass distribution and periodicity that suggests a molecular basis for structural flexibility. *Eur. J. Pediatr.* 155:734–735.

36. Sherratt, M.J., D.F. Holmes, C.A. Shuttleworth, and C.M. Kielty. 1997. Scanning transmission electron microscopy mass analysis of fibrillin-containing microfibrils from foetal elastic tissues. *Int. J. Biochem. Cell Biol.* 29:1063–1070.

37. Siracusa, L.D., M.R. McGrath, Q. Ma, J.J. Moscow, J. Manne, P.J. Christner, A.M. Buchberg, and S.A. Jimenez. 1996. A tandem duplication within the *fibrillin* 1 gene is associated with the mouse *Tight skin* mutation. *Genome Res.* 6:300–313.

38. Taipale, J.J. Saharinen, K. Hedman, and J. Keski-Oja. 1996. Latent transforming growth factor-β-1 and its binding protein are components of extracellular matrix microfibrils. *J. Histochem. Cytochem.* 44:875–889.

39. Witt, D.R., and M.R. Hayden. 1986. Restrictive dermopathy: a newly recognised autosomal recessive skin dysplasia. *Am. J. Med. Genet.* 24:631–648.